Chemical Physics Letters 615 (2014) 83–88

Contents lists available at ScienceDirect

Chemical Physics Letters

journal homepage: www.elsevier.com/locate/cplett

The behaviour of charge distributions in dielectric media

Piet Th. van Duijnen[a], Hilde D. de Gier[a], Ria Broer[a], Remco W.A. Havenith[a,b,c,*]

[a] Theoretical Chemistry, Zernike Institute for Advanced Materials, University of Groningen, Nijenborgh 4, 9747 AG Groningen, The Netherlands
[b] Stratingh Institute for Chemistry, University of Groningen, Nijenborgh 4, 9747 AG Groningen, The Netherlands
[c] Ghent Quantum Chemistry Group, Department of Inorganic and Physical Chemistry, Ghent University, Krijgslaan 281 – (S3), B-9000 Gent, Belgium

ARTICLE INFO

Article history:
Received 19 June 2014
In final form 1 October 2014
Available online 13 October 2014

ABSTRACT

Screened Coulomb interaction in dielectrics is often used as an argument for a lower exciton binding energy and easier exciton dissociation in a high dielectric material. In this paper, we show that at length scales of excitons (10–20 Å), the screened Coulomb law is invalid and a microscopic (quantum chemical) description is necessary to describe the medium effect on exciton dissociation. The exciton dissociation energy decreases with increasing dielectric constant, albeit deviating from the inversely proportional relationship. The electron–hole interaction energy, approximated with a point charge model, is apparently not affected by the dielectric constant of the environment.

1. Introduction

In the quest for more efficient organic photovoltaic devices (OPVs), the use of materials with a high dielectric constant has been suggested [1]. One reason why organic photovoltaic systems are less efficient than inorganic solar cells like those based on silicon, is the high exciton binding energy. This is commonly attributed to the low dielectric constant of OPVs ($\varepsilon \approx 4$) [2,3]. This idea is based on the screened Coulomb law in ponderable materials, which tells us that the interaction energy and force between point charges embedded in such media are given by, respectively (in atomic units),

$$U_{ij} = \frac{Q_i Q_j}{\varepsilon R_{ij}}$$
$$\mathbf{F}_{ij} = \frac{Q_i Q_j (\mathbf{R}_j - \mathbf{R}_i)}{\varepsilon R_{ij}^3}; \quad \varepsilon \geq 1.0 \tag{1}$$

with Q_i and Q_j the point charges, $\mathbf{R}_i$ and $\mathbf{R}_j$ their positions, R_{ij} the distance between them and ε the (relative) dielectric constant of the medium. By definition, $\varepsilon \geq 1.0$, furthermore, ε is independent of the type (plus or minus) of the charges, which means that like (+/+, or −/−) and unlike (+/−) interactions are equally reduced as compared to the vacuum situation ($\varepsilon = 1.0$). A charge Q_i in a cavity of radius a, embedded in an infinite continuum with dielectric constant ε, gives rise to an induced charge on the cavity's surface (Born formula [4]):

$$Q_i^* = -\left(1 - \frac{1}{\varepsilon}\right) Q_i \tag{2}$$

which is independent of a. When a second charge (Q_j) is introduced, at a distance R_{ij} so large that the total interaction energy, to first order, can be written as [5]

$$U_{ij} = \frac{1}{R_{ij}} \left[Q_i Q_j + \frac{1}{2}(Q_i^* Q_j + Q_i Q_j^*) \right] \tag{3}$$

i.e., if the polarisation comes only from the inducing charges separately without cross terms, then Eq. (2) can be inserted in Eq. (3) giving Eq. (1).

Hence, Eq. (1) holds only for *macroscopic* situations, *i.e.*, the charges are averages over macroscopic volumes, although small with respect to the actual size of the system, and therefore should be at *macroscopic* distances (at least about 100 Å [6]) from each other. However, an exciton generated in OPV materials consists of a pair of unlike charges at a separation of 10–20 Å in a molecular, and therefore highly anisotropic, polarisable environment. As a consequence, Eq. (1) should not be used to describe or explain the charge separation: the charges must already be farther separated before the screened Coulomb law is applicable. Hence, it is not straightforward that the charges involved in an exciton behave like they were in a macroscopic dielectric, and a more indepth consideration of their behaviour is necessary to understand charge separation in OPVs better. Therefore, in this contribution, the effective forces between charges and exciton binding energies are studied in different materials, and the consequences for OPVs are discussed.

* Corresponding author at: Theoretical Chemistry, Zernike Institute for Advanced Materials, University of Groningen, Nijenborgh 4, 9747 AG Groningen, The Netherlands.
E-mail address: r.w.a.havenith@rug.nl (R.W.A. Havenith).

http://dx.doi.org/10.1016/j.cplett.2014.10.003
0009-2614/

The paper is structured as follows: below a short overview is given of studies that are relevant for the topic at hand. In Section 2 the behaviour of point charges in inorganic C and Si clusters is discussed, because the dielectric constants of these materials are known. Subsequently, in Section 3, the dissociation of point charges is modelled in different organic materials. The materials are selected based on their different properties: one is a reference alkane, one material contains dipoles, and one material contains highly polarisable atoms. These materials can serve as side-chains in organic photovoltaic polymers to enhance the dielectric constant. In Section 4, the influence of a dielectricum on the exciton binding in a typical donor–acceptor complex is investigated. In Section 5, the findings of the previous sections are combined for a typical photovoltaic system [7] to investigate the effect of the dielectric constant on the exciton binding energy. Finally, in Section 6, a summary is given of the most important conclusions: the screened Coulomb law is not applicable for the description of an arbitrary collection of charges and polarisabilities and microscopic studies using QM/MM methods are necessary to investigate the effect of the medium on the exciton dissociation.

As early as 1982, Van Duijnen and Thole [8] noted that a dielectric placed *between* two interacting charges increases the interaction ($\varepsilon_{eff} < 1.0$). Later, Rullmann et al. [9] showed that microscopic collections of (point) charges and polarisabilities show behaviour that cannot be described by the simple expression of Eq. (1), while De Vries and Van Duijnen [10] discussed the problems associated with mixing macroscopic and microscopic descriptions of such systems. In microscopic studies where deviations from Eq. (1) were found — charges interacting more than *in vacuo* ($\varepsilon_{eff} < 1.0$), even like charges attracting each other ($\varepsilon_{eff} < 0.0$) — were reported [11–13].

In most efforts for calculating exciton binding energies by applying the Bethe-Salpeter equation the interaction is screened with the (bulk) dielectric constant for interaction distances [14,15] well below the 100 Å mentioned above. Interestingly, Deslippe et al. [16] reported exciton interactions in carbon nanotubes, larger than 'bare' interactions, which they coined 'anti-screening'.

A frequently recurring picture is that of a Coulomb potential like Eq. (1) with indications of the interaction between charges in a dielectricum. Gregg and Hanna [17] suggest that the strong interaction in excitons is caused by the small dielectric constant in typical OPVs ($\varepsilon \approx 4$), in contrast with the free electron-hole pairs in inorganic semiconductors ($\varepsilon \approx 15$). In 2004, Gregg et al. [18] put this even stronger: "Thus, increasing ε ... leads to a greater average distance between the charges." But there is also a warning: "Finally, ε is a bulk quantity and is valid only over distances of many lattice spacings; ..." Unfortunately, in following papers, this warning is absent, and in the recent review of Clarke and Durrant [2] the dielectric constant is still a very important parameter, and the Onsager model, or more recently developed versions [19–23] of it, is still the main [1] operative theory. [24] In all these works the expected effect of the dielectric constant (or the permittivity) comes from model calculations based on the Onsager model.

Lately, an increasing number of studies have been reported in which microscopic descriptions are used for specific systems [25–31]. However, also there the importance of the dielectric constant is (often) mentioned [1,24,25].

2. Dielectric or not?

Recently Van Duijnen and Swart reported a Discrete Reaction Field (DRF) [32] study on Si_n-clusters [33] (n ranging from 3 to ~5000) in which they arrived from first principles at the experimental dielectric constant for the larger clusters ($n = 1750, 4950$). In a correct treatment of the many-body polarisation in an arbitrary collection of point charges and polarisabilities, the induced dipole μ_p in the polarisable point p is determined by the local field, *i.e.*, the sum of the external field and the fields, t_{pq}, of all dipoles induced elsewhere:

$$\mu_p = \alpha_p[E_p^0 + \sum_{q \neq p} t_{pq}\mu_q] \tag{4}$$

E^0 consists of any applied field plus the field of any charge distribution in the system [34–39]. The dipole–dipole interaction tensors t_{pq} in Eq. (4) contain only geometric parameters.

Hence, it is through the mutual orientation and distances that the polarisable particles respond differently in various (local) structures, which in the end makes the results sometimes counter-intuitive and cannot be caught in the simple form of Eq. (1).

In DRF, the two-particle interactions are damped at short distances in order to avoid too large and unphysical results [34,40]. The electric potentials, fields and field gradients of charges are damped in a consistent way and the damped fields and dipole–dipole tensors are the derivatives of the potential and the field, respectively [32]. Eq. (4) for the many-particle problem can be put into matrix form:

$$\mathbf{M} = \mathbf{B}\mathbf{E}^0 = [\mathbf{A}^{-1} - \mathbf{T}]^{-1}\mathbf{E}^0 \tag{5}$$

in which $\mathbf{M}$ is the vector of (self-consistent) induced dipoles, $\mathbf{E}^0$ the vector of the initial field, $\mathbf{A}$ the block-diagonal matrix of the (vacuum) polarisabilities, and $\mathbf{T}$ the (off-diagonal) interaction tensors. Hence, $\mathbf{B}$ is a normal (but many-body) polarisability thus leading to an induction energy:

$$U_{ind} = -\frac{1}{2}\mathbf{E}^0\mathbf{B}\mathbf{E}^0 \tag{6}$$

By applying unit fields in x-, y- and z-directions, the *effective* mean polarisabilities are obtained from Eq. (5). We note here that the $\mathbf{T}$-blocks in the condensed phases generally lead to effective local polarisabilities that are *smaller* than the vacuum values [33].

Reversely, by fitting Eq. (5) to (experimental or calculated) molecular polarisabilities, the vacuum, or 'free-atom' polarisabilities $\{\alpha_p\}$ are obtained. With these ('input') parameters the polarisabilities of molecules – not belonging to the learning sets – are calculated from Eq. (5) with experimental accuracy [41]. Typically, each 'free' atomic polarisability is independent of its 'chemical environment': the latter is in all cases absorbed in the $\mathbf{T}$-blocks of $\mathbf{B}$.

In Figure 1, the average (per atom) mean polarisablities of the atoms of a cluster consisting of 4950 atoms of carbon and silicon in

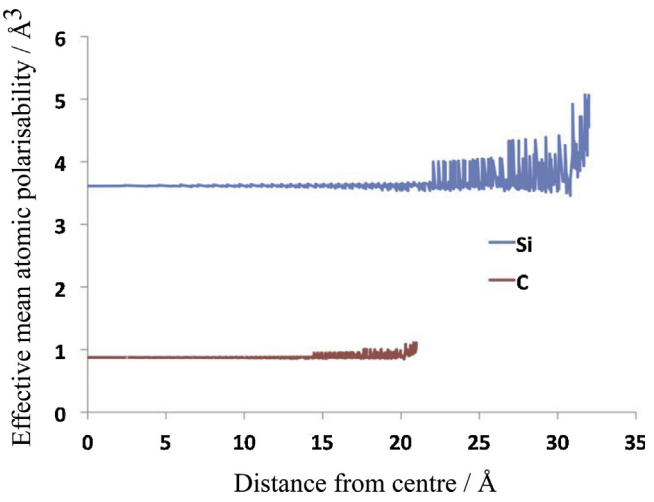

Figure 1. Effective atomic polarisability of C and Si in C/Si_{4950}-clusters in their experimental (diamond) structures as a function of the distance to the centre.

Table 1
Forces (au) between charged atoms (1.0 au) in Si_{4950}, about 46 Å apart, by finite differences.

	+/−	+/+
F_{elst}	-0.132×10^{-3}	0.132×10^{-3}
F_{ind}	-0.357×10^{-3}	-0.502×10^{-3}
F_{total}	-0.489×10^{-3}	-0.370×10^{-3}
ε_{eff}	0.27	−0.36

F_{elst} = electrostatic (unscreened) force. F_{ind} = force due to induction, F_{total} = total force, $\varepsilon_{eff} = F_{vac}/F_{total}$. For details, see Table S1.

their experimental (diamond) structures are plotted as a function of their distance to the centre of the (roughly spherical) clusters. For silicon, the 'free atom' polarisability ($\alpha_{Si} = 5.9$ Å^3) was obtained from the calculated polarisability [42] of Si_3, while for carbon the default value in DRF90 was used ($\alpha_C = 1.3$ Å^3), which came from a fit to a learning set of 52 molecules [40].

We note that the calculated average atomic polarisability in the interior is substantially smaller than the input value. This is caused by the local field contributions of the induced dipoles in the environment. Since there are no induced (counteracting) dipoles outside the edge of the clusters, the mean polarisabilities there are larger. For Si, $\alpha^{eff} = 3.72$ Å^3 is in perfect agreement with the value obtained from the Clausius–Mossotti relation:

$$\alpha = \frac{3}{4\pi}\frac{\varepsilon - 1}{\varepsilon + 2}\Omega = \frac{\varepsilon - 1}{\varepsilon + 2}\langle r\rangle^3 \tag{7}$$

where Ω is the average atomic volume, $\langle r\rangle$ the average atomic radius, and ε the dielectric constant. The atomic radii were obtained from the volumes of the unit cells. From the simulations, $\varepsilon_{Si} = 12$ and $\varepsilon_C = 6$ were found, for which the experimental values are 11.8 and 5.5, respectively.

Although the calculated dielectric constants are in good agreement with experiment, the question is whether these clusters behave as real dielectrics. In order to check this, the force between two charged cluster atoms (each with $|Q| = 1$ au), about 46 Å apart in the Si_{4950} cluster was calculated from finite differences (Table 1).

The two effective dielectric constants calculated are far away from $\varepsilon = 12$, because the polarisation *between* the charges is different from that *outside*, which is called 'local asymmetry' [12]. This situation clearly violates Eq. (3) and hence Eq. (1). Also, the induced dipole moments for like and unlike charges are different. For example, on the line connecting the two charges, the moments for like charges counteract and therefore almost cancel, while for unlike charges they reinforce each other. Hence the difference in scaling and, again, a violation of Eq. (3). In fact, on averaging the charge over the volume in this system, the total charge would be zero, and no polarisation would occur outside its volume.

In Figure 2, the dipoles induced by a unit charge in the centre of the system displayed in Figure 1 is depicted as a function of the atom distance to the origin. Imagine a system consisting of two just touching Si_{4950}-clusters, *i.e.*, with a distance between the charges of about 80 Å. Then we would have a system that fulfil approximately the requirements for applying Eq. (1): the local environment and polarisation of each of the charges is practically identical and in between them the induction vanishes.

3. Modelling exciton dissociation in different materials

In the preceding section we treated two point charges at specific geometries and different distances. In the present section, the dissociation of two oppositely charged point particles ($Q = \pm 1$ au) is studied in a rectangular box ($a = 20$ Å, $b = 20$ Å, $c = 40$ Å) filled with nonane (**1**, 82 molecules, $\rho = 1.09$ g/ml), 1-methoxy-2-(2-methoxyethoxy)ethane (**2**, 78 molecules, $\rho = 1.09$ g/ml), and with 1,8-diiodooctane (**3**, 48 molecules, $\rho = 1.82$ g/ml), respectively. The

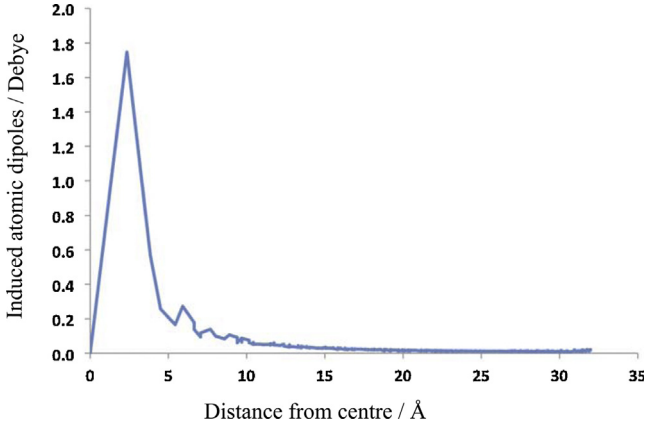

Figure 2. Dipoles induced by one unit charge positioned in the origin of the Si_{4950}-cluster.

distance between the charges was varied between 2 Å and 30 Å in the *c*-direction, and the force between the charges was calculated by numerical differentiation (at each distance, the molecules in the box were allowed to relax (MM3 force field [43])). After relaxation, the molecules in the box were treated both fully quantum mechanically (HF/6-31G) and using the DRF force field (GAMESS-UK [44]). The force as a function of the distance is plotted in Figure 3. It is evident from Figure 3 that these clusters of molecules do not behave like dielectric media. The forces between the charges do not vary smoothly with distance and they deviate considerably from Eq. (1).

A comparison between the HF and DRF calculated forces shows for both methods similar trends, the DRF curve is, however, more extreme in the deviations from ideal behaviour, because the DRF response is basically linear, while for electrons at short distances the response is nonlinear. In all three media regions exist where the charges attract each other more than in vacuum and regions where they even repel each other. At very short distances (<5 Å), the Coulombic force between the two charges is effectively reduced by the presence of the medium, but no dielectric *constant* emerges.

At intermediate distances (10–25 Å), **2** seems to favour exciton dissociation. The other compounds, **1** and **3**, show the same behaviour, but at longer distances (>25 Å). Compound **2** shows at these distances attraction of the charges again. However, the irregular shape of the curves is presumably very dependent on the orientation of the molecules surrounding the charges, thus conclusions regarding which medium would enhance exciton dissociation cannot be drawn from this study. What is shown by this model study is that for distances of 2–30 Å between charges, no unique dielectric constant can be defined, and exciton dissociation has to be studied using microscopic (quantum chemical) methods.

4. The effect of a dielectricum on exciton binding in a donor–acceptor complex

In Figure 4, we present a typical molecular donor–acceptor complex (**4**), which is a monomer of a polymer often used in OPVs, for which we calculated the spectrum with the INDOs/CIS package [45], extended with the DRF force field for QM/MM applications [46–48] *in vacuo*, and embedded in Si_{4950} or C_{4950}, respectively. In the latter cases, first the centres of mass of the cluster and **4** were made coincident and then the cluster atoms that are too close (distance smaller than the sum of the Van der Waals radii) to the monomer were deleted (Fig. S1).

The CI active space contained the orbitals ranging from HOMO-10 to LUMO + 9 (in total 21 active orbitals), and we calculated the lowest five roots of the CI-matrix, giving the lowest excited state (S_1) at ~2.7 eV. From the excitation energy, the ionisation energy

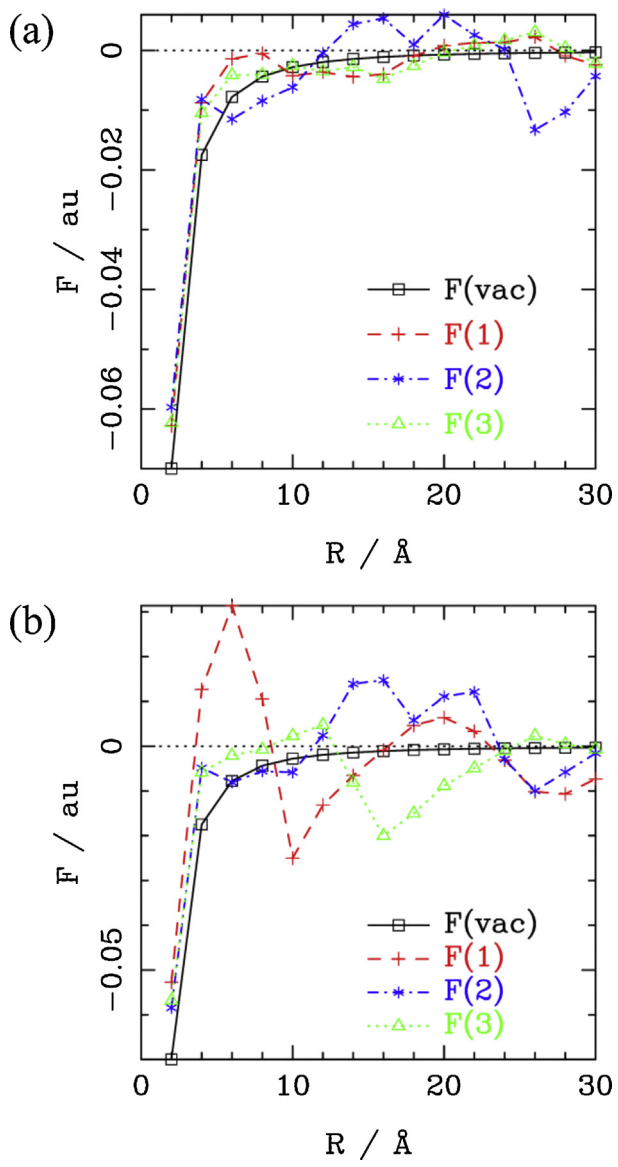

Figure 3. The force (au) between a plus and a minus charge as a function of their distance (Å) in nonane (**1**), 1-methoxy-2-(2-methoxyethoxy)ethane (**2**), and 1,8-diiodooctane (**3**), respectively. In a), the molecules are treated with HF/6-31G, in b) the molecules are treated with the DRF approach. For comparison, the force in vacuum is also plotted.

(IP), and the electron affinity (EA), we arrive at the exciton dissociation energy, E_{diss} = IP-EA-$E_{excitation}$, which is often called the exciton binding energy. In order to obtain an estimate of the interaction energy between the excited electron charge distribution and the cation left behind (E_{int}), we first constructed a (Mulliken) point

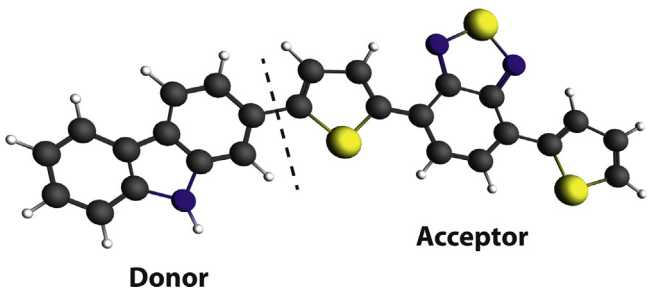

Figure 4. The donor–acceptor complex **4**.

Table 2
Energies (eV) and forces (au) in complex **4** in various environments.

Energy	Environment		
	Vac	C	Si
IP	7.07	6.78	6.25
EA	2.22	2.56	3.22
$E_{excitation}$	2.67	2.55	2.24
E_{diss}	2.18	1.67	0.79
E_{int}	−6.83	−6.78	−6.79
Force	0.0729	0.0733	0.0770

charge representation of the ground state charge distribution. Next, a representation of an effective 'electron' distribution was constructed, by first making a linear combination of the MOs describing the excited electron, using the appropriate CI coefficients. Then the Mulliken analysis was applied. The 'hole' distribution was obtained by the same procedure for the singly occupied MOs from which the electron was excited. The 'cation' distribution was calculated by subtracting the 'hole' distribution from the ground state charge distribution. Finally, of all distributions the centre of charge was determined (Table S2 and Fig. S2). Since these point charges represent all polarisations, in both the ground and excited state, a reasonable estimate of E_{int} is computed from simple Coulomb interactions between the 'electron' and the 'cation' point charges. By moving the centre of the electron distribution by ±0.01 Å along the line connecting its centre to that of the cation distribution, we arrive at the force with which the electron is held. In Table 2 the results are summarised (see also Table S3).

From Table 2, we see that in all cases the dissociation energy, E_{diss}, behaves more or less as expected with respect to the environment: it decreases as the dielectric constant increases, albeit not inversely proportional to ε. This is not surprising: this physical quantity involves removing an electron from a site, and adding it to another site so far away that no hole–electron interaction occurs. In contrast, the exciton interaction energy, E_{int}, is virtually not affected by the presence of a dielectric environment. It is this entity that, *e.g.*, in the Bethe–Salpeter formalism, often is divided by the (bulk) dielectric constant, thus leading to too small values for E_{int}, and possibly to wrong charge distributions [7,14,15]. This practice is not only unwarranted because of the too small electron–hole distance, but also because the scaling in these cases is not appropriate. The $1/\varepsilon$ behaviour belongs to completely dissociated (point) charges, while a microscopic description of the systems at hand requires a reaction field approach like ours, which scales quite differently. The forces are in all cases positive (repulsive), and show, like the interaction energies, no connection with the dielectric constant of the environment.

5. OPV efficiency and permittivity in practice

In a recent study [7] it is argued that the exciton *binding* energy was lowered by increasing the permittivity of thin films of B,O-chelated azadipyrromethene (BO-ADPM, Fig. S3) blended with camphoric anhydride (CA, Fig. S4), and thereby increasing the OPV efficiency. The authors measured an increased internal quantum efficiency of ~30%, and related it to an increase of the dielectric constant from ~4.5 to ~11. In the light of the findings presented here, a more elaborate explanation than that based on Eq. (1) must be given to rationalise their results, because the hole–electron distance is far too small to be affected by the dielectric medium. Furthermore, only tiny changes in the absorption spectrum in the various mixtures are observed, suggesting that the interaction between BO-ADPM and CA is very weak. To confirm these experimental findings, we performed a number of INDOs/DRF/CIS [33] calculations, with the standard INDOs parameterisation [45], to obtain the

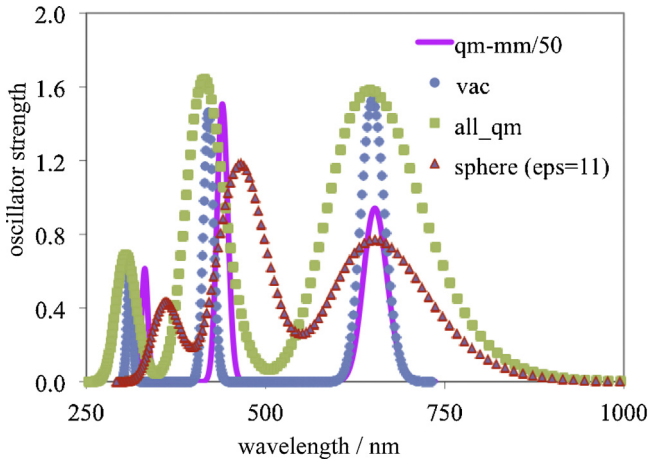

Figure 5. Absorption spectra of BO-ADPM. The blue (circles) curve shows the spectrum of BO-ADPM *in vacuo*, the red (triangles) curve shows the spectrum of BO-ADPM in a spherical cavity with $r = 22$ Bohr embedded in a dielectric continuum with $\varepsilon = 11$, the purple (solid line) one shows the spectrum of 50 uncorrelated structures obtained by MD calculations with DRF90 on one BO-ADPM molecule surrounded by ten CA molecules, and the green (diamonds) one shows the spectrum obtained by an all QM calculation of the spectrum of BO-ADPM$(CA)_{10}$ in the solute/solvent configuration mentioned in the main text.

lowest BO-ADPM excitation energy. The experimental spectrum consists of bands around 325, 500 and 750 nm (3.8, 2.5 and 1.6 eV).

The calculated ground state vacuum dipole moment of BO-ADPM was found to be 1.31 Debye (0.51 au) and applying the Born formula [4] (Eq. (8)) we obtained a first estimate of the solvation energy of this dipole (μ) in a spherical cavity with radius r:

$$\Delta G_{solv} = -\frac{1}{2} r^{-3} \frac{2(\varepsilon - 1)}{1 + 2\varepsilon} \mu^2 \tag{8}$$

For a hole–electron dipole of 0.51 au in a sphere with $r = 22$ Bohr, *i.e.*, a sphere just containing the BO-ADPM molecule, placed in a continuum with $\varepsilon = 11$, we get $G_{solv} \approx -1.1 \times 10^{-5}$ Hartree (-3×10^{-4} eV).

Considering the Born formula to be a too crude approximation, we used again the INDOs/CIS/DRF [45,47] method to calculate the spectrum of BO-ADPM in a sphere of the same size applying the Boundary Element Method (BEM) [49], and calculated the interaction with the continuum and the absorption spectrum, using the standard INDOs parameterisation. The calculated spectrum (red curve (triangles) in Figure 5) is very similar to the experimental one, apart from a blue shift of about 100 nm (0.25 eV) of the experimental 750 nm band. The ΔG_{solv} (INDO/DRF) $= -2.2 \times 10^{-4}$ Hartree (-6×10^{-3} eV) is larger than obtained from Eq. (8) by going beyond the point dipole approximation for the charge distribution. For the exciton dissociation energy (see above), we got E_{diss}(vac) = 1.71 eV and $E_{diss}(\varepsilon = 11, r = 22$ Bohr$) = 0.55$ eV. This is indeed smaller than *in vacuo*, but not related like in Eq. (1).

To further improve on the calculation of media effects on the absorption spectrum and the exciton binding energy, we performed some MD calculations with DRF90 on one BO-ADPM molecule surrounded by ten CA molecules, and collected 50 uncorrelated structures from which 50 spectra were calculated. A total of 750 excitation energies were sorted in 3 boxes of width 0.91 eV (the difference of the smallest and largest excitation energy divided by the number of boxes, thus defining the resolution) and adding the oscillator strengths within each box. The results in the boxes were convoluted with Gaussians of width 0.27 eV. The resulting spectrum (purple curve (solid line) in Figure 5) in the visible region differs again not significantly from the computed vacuum spectrum. The mean ground state interaction energy with the environment was 8×10^{-4} ($\pm 6 \times 10^{-4}$) Hartree (0.022 ± 0.016 eV). The

Table 3
Energies (eV) and forces (au) in BO-ADPM in various environments.

Energy	Environment			
	Vac	Sphere	Si	CA_{10} (qm)
IP	5.86	5.25	5.09	5.63
EA	2.24	2.80	3.09	2.23
$E_{excitation}$	1.91	1.90	1.91	1.92
E_{diss}	1.71	0.55	0.09	1.48
E_{int}	−6.35	−6.35	−6.36	−6.35
F	−0.0066	−0.0315	−0.0214	−0.0439

exciton dissociation energy obtained from a single 'solute/solvent' configuration is 1.46 eV, *i.e.*, slightly lower than the vacuum exciton binding energy, but even farther from the supposed relation *via* Eq. (1). Finally, we performed an all QM calculation of the spectrum of BO-ADPM$(CA)_{10}$ in the solute/solvent configuration mentioned above. Again, no significant differences were obtained: the same spectrum (green curve (diamonds) in Figure 5), E_{diss} (1.46 eV), and ground state dipole moment (10.01 D) were found, in perfect agreement with the ensemble average of the MD calculations (9.95 D).

Also the dielectric constant of the system BO-ADPM$(CA)_{10}$ was calculated following the same procedure as above by applying Eq. (5) with averaged induced dipoles on each atom and averaged radii. We arrived at $\varepsilon_{eff} = 1.51$, while the ratio between the averaged dissociation energy in the cluster and in vacuum gives $\varepsilon_{eff} = 1.16$, and this ratio for E_{int} is smaller than one.

Finally, we 'solvated' BO-ADPM with our Si-cluster with its dielectric constant of 12. In Table 3 (see also Table S6), an expected pattern emerges: indeed E_{diss} is reduced strongly, in contrast with the behaviour of E_{int}, which is in all cases the same.

Interestingly, the CA-environment never shows an effect that possibly can be related with $\varepsilon \approx 11$, in contrast with the Si-cluster. This, and the fact that interaction of BO-ADPM with CA is very weak, more than the dielectric effects is needed to explain the behaviour of the BO-ADPM(CA) system.

6. Conclusions

This study shows that application of the screened Coulomb law modified for dielectrics cannot be used to describe the interaction between charges at the microscopic level. Thus, it is not obvious that increasing the dielectric constant of the medium alone is sufficient to yield more efficient OPV devices. Microscopic studies using QM/MM methods are necessary to investigate the effects of the medium on exciton *interaction* energy, *i.e.*, the interaction between an excited electron and the cation it leaves behind. This strategy has also been underlined recently in a review of Chiechi et al. [50] Only for the exciton *dissociation* energy (E_{diss}), a relation with the system's dielectric constant can be found, albeit deviating from the inversely proportional relationship with ε.

Acknowledgments

The authors thank the reviewers for their constructive comments. R.W.A.H. acknowledges the Zernike Institute for Advanced Materials ("Dieptestrategie" program) for financial support. This work is part of the research programme of the Foundation of Fundamental Research on Matter (FOM), which is part of the Netherlands Organisation for Scientific Research (NWO). This is a publication of the FOM-focus Group 'Next Generation Organic Photovoltaics', participating in the Dutch Institute for Fundamental Energy Research (DIFFER). The work was partially done with computing time at the Dutch National Supercomputer Cartesius (SURFsara, SH-213-13).

Appendix A. Supplementary data

Supplementary data associated with this article can be found, in the online version, at doi:10.1016/j.cplett.2014.10.003.

References

[1] L.J.A. Koster, S.E. Shaheen, J.C. Hummelen, Adv. Energy Mater. 2 (2012) 1246.
[2] T.M. Clarke, J.R. Durrant, Chem. Rev. 110 (2010) 6736.
[3] S.E. Gledhill, B. Scott, B.A. Gregg, J. Mater. Res. 20 (2005) 3167.
[4] M. Born, Z. Phys. 1 (1920) 45.
[5] R. Constanciel, Theor. Chim. Acta 69 (1986) 505.
[6] J.D. Jackson, Classical Electrodynamics, John Wiley & Sons, New York, 1975.
[7] S.Y. Leblebici, T.L. Chen, P. Olada-Velasco, W. Yang, B. Ma, ACS Appl. Mater. Interfaces 5 (2013) 10105.
[8] P.Th. van Duijnen, B.T. Thole, Biopolymers 21 (1982) 1749.
[9] J.A.C. Rullmann, M.N. Bellido, P.Th. van Duijnen, J. Mol. Biol. 206 (1989) 101.
[10] A.H. de Vries, P.Th. van Duijnen, A.H. Juffer, Int. J. Quantum Chem, Quantum Chem. Symp. 27 (1993) 451.
[11] C. Jarque, A.D. Buckingham, Chem. Phys. Lett. 164 (1989) 485.
[12] P.Th. van Duijnen, A.H. de Vries, Int. J. Quantum Chem, Quantum Chem. Symp. 29 (1995) 523.
[13] R. Zangi, J. Chem. Phys. 126 (2012) 184501.
[14] J.-W. van der Horst, P.A. Bobbert, M.A.J. Michels, H. Bässler, J. Chem. Phys. 114 (2001) 6950.
[15] O. Lehtonen, D. Sundholm, T. Vänskä, Phys. Chem. Chem. Phys. 10 (2008) 4535.
[16] J. Deslippe, M. Dipoppa, D. Prendergast, M.V.O. Moutinho, R.B. Capaz, S.G. Louie, Nano Lett. 9 (2009) 1330.
[17] B.A. Gregg, M.C. Hanna, J. Appl. Phys. 93 (2003) 3605.
[18] B.A. Gregg, S.-G. Chen, R.A. Cormier, Chem. Mater. 16 (2004) 4586.
[19] K.M. Hong, J. Noolandi, J. Chem. Phys. 69 (1978) 5026.
[20] M. Tachiya, J. Chem. Phys. 89 (1988) 6929.
[21] V.D. Mihailetchi, L.J.A. Koster, J.C. Hummelen, P.W.M. Blom, Phys. Rev. Lett. 93 (2004) 216601.
[22] V.D. Mihailetchi, L.J.A. Koster, P.W.M. Blom, C. Melzer, B. de Boer, J.K.J. van Duren, R.A.J. Janssen, Adv. Funct. Mater. 15 (2005) 795.
[23] M. Wojcik, M. Tachiya, Rad. Phys. Chem. 74 (2005) 132.
[24] M. Lenes, et al., J. Appl. Phys. 104 (2008) 114517.
[25] G. D'Avino, et al., J. Phys. Chem. C 117 (2013) 12981.
[26] D. Beljonne, J. Cornil, L. Muccioli, C. Zannoni, J.-L. Brédas, F. Castet, Chem. Mater. 23 (2011) 591.
[27] S.R. Yost, L.-P. Wang, T. van Voorhis, J. Phys. Chem. C 115 (2011) 14431.
[28] J.-L. Brédas, J.E. Norton, J. Cornil, V. Coropceanu, Acc. Chem. Res. 42 (2009) 1691.
[29] J. Cornil, et al., Acc. Chem. Res. 46 (2013) 434.
[30] S.M. Ryno, S.R. Lee, J.S. Sears, C. Risko, J.-L. Brédas, J. Phys. Chem. C 117 (2013) 13853.
[31] N. Gorczak, M. Swart, F.C. Grozema, J. Mater. Chem. C 2 (2014) 3467.
[32] M. Swart, P.Th. van Duijnen, Mol. Simul. 32 (2006) 471.
[33] P.Th. van Duijnen, M. Swart, J. Phys. Chem. C 114 (2010) 20547.
[34] B.T. Thole, Chem. Phys. Lett. 59 (1981) 341.
[35] L. Silberstein, Philos. Mag. 33 (1917) 521.
[36] J. Applequist, Acc. Chem. Res. 10 (1977) 79.
[37] R.W. Munn, T. Luty, Chem. Phys. 81 (1983) 41.
[38] R.W. Munn, Chem. Phys. 50 (1980) 119.
[39] Z.G. Soos, E.V. Tsiper, R.A. Pascal Jr., Chem. Phys. Lett. 342 (2001) 652.
[40] P.Th. van Duijnen, M. Swart, J. Phys. Chem. A 102 (1998) 2399.
[41] M. Swart, P.Th. van Duijnen, J.G. Snijders, J. Mol. Struct. (Theochem) 458 (1999) 11.
[42] C. Pouchan, D. Begue, D.Y. Zhang, J. Chem. Phys. 121 (2004) 4628.
[43] N.L. Allinger, Y.H. Yuh, J.-H. Lii, J. Am. Chem. Soc. 111 (1989) 8551.
[44] M.F. Guest, et al., Mol. Phys. 103 (2005) 719.
[45] M.C. Zerner, in: K.B. Lipkovitz, D.B.N. Boyd (Eds.), Reviews of Computational Chemistry, VCH, New York, 1991, p. 313.
[46] P.Th. van Duijnen, T.L. Netzel, J. Phys. Chem. A 110 (2006) 2204.
[47] P.Th. van Duijnen, M. Swart, L. Jensen, in: S. Canuto (Ed.), Solvation Effects on Molecules and Biomolecules: Computational Methods and Applications, Springer, 2008, p. 39.
[48] L. van het Goor, P.Th. van Duijnen, C. Koper, L.W. Jenneskens, R.W.A. Havenith, F. Hartl, J. Solid State Electrochem. 15 (2011) 2107.
[49] P.Th. van Duijnen, A.H. Juffer, J.P. Dijkman, J. Mol. Struct. (Theochem) 260 (1992) 195.
[50] R.C. Chiechi, R.W.A. Havenith, J.C. Hummelen, L.J.A. Koster, M.A. Loi, Mater. Today 16 (2013) 281.